ENVIRONMENTAL RESEARCH
LETTERS

LETTER • OPEN ACCESS

Two decades of aerosol trends over India: seasonal characteristics and urban-rural dynamics

To cite this article: Prathmesh Namdeo *et al* 2024 *Environ. Res. Lett.* **19** 124065

ENVIRONMENTAL RESEARCH
LETTERS

OPEN ACCESS

RECEIVED
21 July 2024

REVISED
31 October 2024

ACCEPTED FOR PUBLICATION
14 November 2024

PUBLISHED
5 December 2024

LETTER

Two decades of aerosol trends over India: seasonal characteristics and urban-rural dynamics

Prathmesh Namdeo[1], **TC Chakraborty**[2,*] and **Abhishek Chakraborty**[1,*]

[1] Environmental Science and Engineering Department, Indian Institute of Technology Bombay, Mumbai, Maharashtra, India
[2] Atmospheric, Climate, and Earth Sciences Division, Pacific Northwest National Laboratory, Richland, WA, United States of America
[*] Authors to whom any correspondence should be addressed.

E-mail: tc.chakraborty@pnnl.gov and abhishekc@iitb.ac.in

Keywords: aerosol, satellite, remote sensing, particulate matter, India, urban, rural

Supplementary material for this article is available online

Abstract

India faces significant air quality challenges, with one of the highest air pollution levels of any country in the world. Here, we examine two decades (2001–2019) of both particulate matter ($PM_{2.5}$) concentration and aerosol optical depth (AOD) over the country. Increases are seen between the two decadal averages, for 2001–2010 and 2011–2019, in western India, particularly in the Indo-Gangetic Plain (IGP). IGP region, including Bihar, West Bengal, Jharkhand, and Uttar Pradesh, shows the highest increases in AOD (+0.03, 13%) and $PM_{2.5,\,s}$ (+8 μg m^{-3}). Seasonal AOD patterns fluctuate, with the IGP experiencing the highest wintertime increase, especially in Bihar (+0.07). In summer, there are increases in AOD along the southern and eastern coastal areas. Monsoons cause a slight rise in AOD, except in Rajasthan. In the post-monsoon season, the IGP experiences a notable increase in AOD (+0.057, 25%), potentially driven by biomass burning in Bihar (+0.11) and Uttar Pradesh (+0.075). Dividing our study area into urban and peri-urban clusters ($n = 2791$), AOD is found to be similar, possibly due to advective mixing. However, the differences between urban and rural areas become more noticeable, especially in the second decade. Correlations between AOD and $PM_{2.5,\,g}$ vary across locations, with the highest found in Kanpur ($R^2 = 0.61$) and weaker in Delhi ($R^2 = 0.42$), highlighting the need for more ground monitoring. However, it suggests that satellite-derived AOD can generally be used to examine trends in $PM_{2.5}$ over longer time frames.

1. Introduction

Air pollution is a significant public health concern, both globally and particularly in India, with major pollution events occurring regularly in heavily populated cities like New Delhi, especially in winter (Ranjan *et al* 2021). Rapid urbanization, which concentrates on human activity and thus the emission of these pollutants, can aggravate local air pollution impacts. While ground-based estimates of air pollution have large sampling biases, satellite data can provide estimates of atmospheric aerosols, which significantly contribute to particulate matter pollution (Vohra *et al* 2021). The spatially continuous nature of satellite-derived aerosols can help us understand their dynamics separately over both urban areas and in their background regions. Beyond health impacts through contributions to ground-level air pollution, atmospheric aerosols can directly impact the Earth's energy balance by scattering and absorbing solar and terrestrial radiation (Chakraborty and Lee 2019), and also indirectly impact the climate by functioning as cloud condensation nuclei and changing the microphysical characteristics of clouds (Ramachandran and Kedia 2013). These impacts of aerosols, crucial for constraining future climate projections, remain uncertain due to limited regional and temporal data on their concentration and properties.

Satellites primarily estimate the radiative impact of aerosols through columnar measures of Aerosol Optical Depth (AOD). AOD is the bulk radiative impact of all aerosols present in a vertical air column from the Earth's surface to the top of the atmosphere (Musonda *et al* 2022). Primary sensors for AOD measurements are Moderate Resolution Imaging Spectroradiometer (MODIS), Multi-angle Imaging Spectroradiometer (MISR), Visible Infrared Imaging Radiometer Suite (VIIRS), etc. In this study, we utilize AOD data from MODIS observations and ground-based PM monitors to analyze spatial (by state) and temporal (from 2001 to 2019) variations in AOD. Given that urban areas can be strong sources of air pollutants due to human activity (Fenger 1999) (Goel *et al* 2017), we hypothesized that urban areas would have stronger air pollution signals than their background areas across spatiotemporal scales. As such, a major motivation for this study is to separately isolate these signals and understand potential urban-rural, as well as peri-urban, variations and spatiotemporal dynamics of atmospheric aerosols in India. No previous study has comprehensively isolated AOD patterns across urban, peri-urban, and rural areas in all of India. Most existing research is limited to specific regions or cities (Vohra *et al* 2021). When national scale assessments of AOD trends have been done, they have not isolated urban and rural signals (Rawat *et al* 2019), (Choudhry *et al* 2012), (Ramachandran *et al* 2012). This highlights a significant gap in understanding the spatiotemporal dynamics of AOD variability in India across urban-rural gradients on a national scale. As such, we focus on how AOD changes over time by season across urban, peri-urban, and rural areas and aim to highlight potential differences in air quality variations between cities and their outskirts in India. Finally, we examine the usefulness of AOD as a proxy for ground-level $PM_{2.5}$ (denoted as $PM_{2.5,\,g}$), finding that AOD generally captures the direction of change in $PM_{2.5,\,g}$.

2. Data and methods

2.1. Estimating AOD across spatial and temporal scales

Satellites can provide a broader perspective on air quality dynamics. Here, we use AOD, indicative of the radiative impact of atmospheric particulate matter, derived from the MODIS sensors onboard NASA's Terra and Aqua satellites (Lyapustin and Wang 2022). The dataset, namely MCD19A2.061, provides daily AOD at 1 km resolution based on the multi-angle implementation of atmospheric correction algorithm (Lyapustin and Wang 2022), ensuring high-quality data through atmospheric correction, cloud and snow masking, viewing geometry corrections, and stringent quality control (Lee *et al* 2011). We use the 'Optical_Depth_055' band of this product, which measures AOD at 0.55 μm, sensitive to aerosol concentrations and atmospheric scattering (Lyapustin and Wang 2022).

Leveraging Google Earth Engine, a cloud-based geospatial processing platform (Gorelick *et al* 2017), we analyze MODIS AOD data from 2001 to 2019 at 1 km resolution. For India, we computed area-weighted state-wise AOD averages, dividing the data into two decades: 2001–2010 (recent past) and 2011–2019 (present), excluding 2020 due to COVID-19 anomalies (Chakraborty *et al* 2021). We also calculated the mean AOD gradient by regressing yearly estimates to reflect changes over the entire period. We conducted the Mann–Kendall test on AOD data from 2001 to 2019 for each state to assess long-term trends and detect any significant changes over time (table S3). Additionally, we conducted a spatial correlation analysis between AOD and $PM_{2.5,\,g}$ concentrations using the finest PM data (15 min temporal resolution) from India's Central Pollution Control Board (CPCB) for 2019 (see more details below). After cleaning the data and calculating annual averages for locations with more than 70% data availability, 114 locations across India were included in the analysis to evaluate the satellite data's effectiveness at representing the spatial variability of ground-level pollution (figure S1).

We also analyzed seasonal AOD variations by calculating average values for Winter (December–February), Summer (March–May), Monsoon (June–September), and Post-Monsoon (October–November), as defined by IMD (Indian Meteorological Department, GOI 2023). To understand rainfall patterns and their influence on AOD, we used the Sub Divisional Monthly Rainfall dataset from 1901 to 2017 (Open Government Data (OGD) Platform India 2022), offering insights into monsoon season rainfall trends.

2.2. Ground-based particulate matter observations

We analyzed $PM_{2.5,\,g}$ concentrations from Continuous Ambient Air Quality Monitoring Stations (CAAQMS), which provide measurements every 15 min. These stations are crucial for local air quality assessment and are accessible via India's Central Pollution Control Board's online platform (CCR 2023).

The gridded surface $PM_{2.5}$ (denoted as $PM_{2.5,\,s}$) dataset by Van Donkelaar *et al* (2021) also provides valuable insights into long-term trends from 1998 to 2021. This dataset uses AOD measurements from NASA's MODIS, MISR, and SeaWiFS (Sea-Viewing Wide Field-of-View Sensor) instruments, combined with the GEOS-Chem chemical transport model is calibrated against global ground observations (Van Donkelaar *et al* 2021). Integrating these datasets allows for a comprehensive understanding of air quality dynamics.

According to the CPCB (CPCB 2023), guidelines, 75%–80% valid data points are required to validate daily or monthly averages. Thus, preprocessing

CAAQMS data CCR (2023) is crucial to eliminate outliers and ensure data integrity. The AirPy data cleaning tool, by Madhumitha *et al* (2023, under review), is used for this purpose. It systematically addresses issues like consecutive repetitions, outliers, negative values, and unit inconsistencies, specifically identifying irregular fluctuations lasting over 24 h. The outliers are detected by flagging values that deviate from the median by more than three times the median absolute deviation (median distance between each observation and the median of all observations), calculated over a 3 h running window. However, it has limitations in handling recurring fluctuations at predefined intervals and discerning genuine ambient conditions.

2.3. Delineating urban-rural regions

To analyze AOD dynamics in urban, peri-urban, and rural regions of India, we first vectorize the medium-density pixels in the Global Human Settlement Layer following Chakraborty *et al* (2021), which generates 2791 urban areas. Then an iterative approach, following the same study, is implemented to create normalized buffers for each urban cluster (figure S2). These surrounding regions are approximately equal in size to the urban clusters they encircle. In the surface urban heat island literature, these buffers are considered rural. However, we call them peri-urban since, unlike surface temperature, which is strongly constrained by local land cover, air pollutants can be advected quite far from the urban proper. The region beyond the peri-urban buffer is considered rural. In terms of area, around 3% of India's total area is considered urban, 3% is considered peri-urban, and the rest is taken as rural (table S2 contains the state-wise fraction of urban/peri-urban area in each state). A total of 32 states (including Union Territories) are found to have data for at least one of the categories: urban, peri-urban, or rural. We then analyze AOD at different timescales (monthly averages and yearly/seasonal changes) for urban, peri-urban, and rural regions. Results are compiled both in aggregate and by state, providing a detailed view of AOD variations across India's diverse regions.

3. Results

3.1. AOD dynamics across space, time and seasons

Distinctive spatial patterns of mean AOD are seen (figures 1 and S3), with the Northern region, including the vast Indo-Gangetic Plain (IGP), occupying nearly 20% of India's geographical area (Vadrevu *et al* 2011) and has a population exceeding 700 million (Dey *et al* 2020), exhibiting notably high AOD (Sharma and Kulshrestha 2014). Between the two decades, the IGP region sees an average increase of +0.03 (around 13%) in AOD, with states like Bihar, West Bengal, Jharkhand, and Uttar Pradesh showing significant increases of +0.069, +0.04, +0.038, and +0.035, respectively (figure 1). The $PM_{2.5,\,s}$ concentrations in Delhi and Haryana exhibit strong changes, increasing by 14 and 10 $\mu g\ m^{-3}$, respectively, while other states see increases ranging from 8 to 10 $\mu g\ m^{-3}$, averaging +8 $\mu g\ m^{-3}$ (figure 1). Despite historically high AOD in IGP, the rate of change of AOD shows a slight reduction (approx. 0.5%) on average in the second decade, and a similar trend is also seen in eastern regions (around 0.2%) (figure S3).

The coastal regions of Gujarat show peak AOD values (+1 AOD levels), indicating elevated aerosol concentrations. The western regions, particularly Rajasthan, display relatively high AOD due to the desert and arid conditions (Sarthi *et al* 2019). Despite its low population density, it registers notably higher pollution levels compared to other regions. The average increase in AOD and $PM_{2.5,\,s}$ levels in the second decade is +0.028 (around 12%) and +3.5 $\mu g\ m^{-3}$, respectively, for western regions. Rajasthan shows a very slight increase in AOD (+0.01), while Maharashtra has the highest increase in both AOD (+0.046) and $PM_{2.5,\,s}$ (+5.1 $\mu g\ m^{-3}$). In terms of the AOD gradient (rate of change of AOD), Gujarat and Rajasthan depict mixed patterns, resulting in an average decrease in the second decade, whereas Maharashtra shows an increasing trend in both AOD and its rate of change.

Conversely, the southern regions have lower AOD, similar to those in the central regions. Overall, the AOD increase in southern states is +0.034 (around 21%). However, the increase in $PM_{2.5,\,s}$ concentrations are relatively less compared to the IGP region, at only +2.5 $\mu g\ m^{-3}$. This indicates that while the increase in AOD in both the IGP and southern regions is of similar magnitude, the changes in $PM_{2.5,\,s}$ concentrations are very different. Telangana has the highest increase in both AOD (+0.054) and $PM_{2.5,\,s}$ (+3.5 $\mu g\ m^{-3}$). A slight increase in the rate of change of AOD is also visible. In the eastern region, AOD has risen, probably significantly influenced by the IGP. Similar increases in AOD are seen in the coastal regions of the east, extending down to the southern states of Andhra Pradesh and Tamil Nadu.

In the winter season (December–February), all regions show an increase in AOD in the second decade, with the highest increase in the IGP (+0.04, around 20%), particularly in Bihar (+0.07) (figures 2(a), (b) , S4 and S5). The seasonal gradient shows an increase in the central and southern regions, while the IGP region experiences a reduced change in the AOD gradient in the second decade (around 0.4%) (figure S6). In the summer (pre-monsoon) season (Mar–May), the northwest region shows a slight decrease (0.02) in AOD in the second decade (figure 2(d)), while all other regions show an increase, with the southern and eastern coastal regions showing significant increases of +0.044 and +0.034, respectively. Odisha and Telangana both have an AOD increase of +0.064. The AOD gradient varied

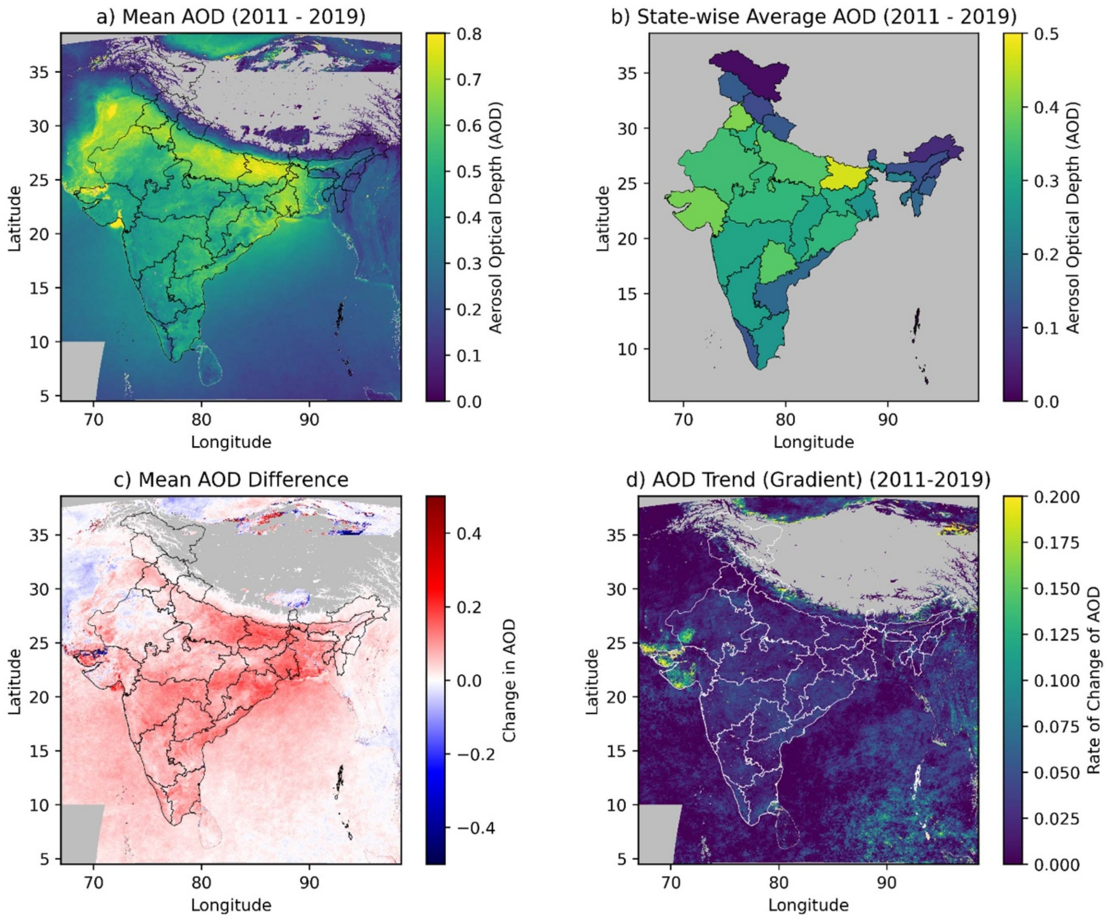

Figure 1. (a) Mean AOD for the year (2011–2019), (b) state-wise average AOD for the year (2011–2019), (c) mean AOD difference between the second decade (2011–2019) and the first decade (2001–2010), (d) rate of change of AOD (AOD Gradient) for the year (2011–2019). (Grey color represents missing data).

greatly across Indian regions (figure S5), with only the eastern and southern regions showing a slight positive change (approx. 0.2%). During the monsoon season (June–September), in the second decade, there is a slight uptick in average AOD across all regions in India except the western region, particularly Rajasthan, where almost no change is observed (figures 2(e) and (f)). The central region shows the highest increase in AOD (+0.035). However, the seasonal gradients show significant variations. Lastly, during the post-monsoon season (October–November), an increase in AOD is observed across India, with the IGP region showing the highest increase (+0.057, 25%) (figures 2(g) and (h)). Bihar marks the highest increase in AOD (+0.11, around 42%), followed by Uttar Pradesh (+0.075, around 30%). The AOD gradient pattern also varies significantly, ranging from −8% to +9%, showing a strong increase (around 6%) in parts of the IGP and central regions and a slight uptick (0.8%) in a small portion of the extreme southern part of Tamil Nadu.

3.2. AOD patterns in urban, peri-urban and rural areas

Examining the AOD for Urban, Peri-Urban, and Rural Areas over the two decades—first (2001–2010) and second (2011–2019)—yields some interesting results. For both Urban and Peri-Urban areas in the second decade, the AOD has increased in the IGP and the eastern coastal regions (Odisha, Andhra Pradesh, Chhattisgarh, Telangana) compared to other regions (central and southern regions) (in figures 3(a) and (b)). Although the AOD is high in the IGP region in the first decade as well, there is an increase in the second decade (+0.062 for urban areas and +0.059 for peri-urban areas). However, the eastern coastal regions show the highest magnitude of increase in AOD in the second decade for both urban (+0.12, 26%) and peri-urban (+0.11, 26%) areas. This increase is significantly higher, as in the first decade, the AOD for the eastern coastal regions is similar in magnitude to the southern and central regions. In rural regions, a significant increase in average AOD

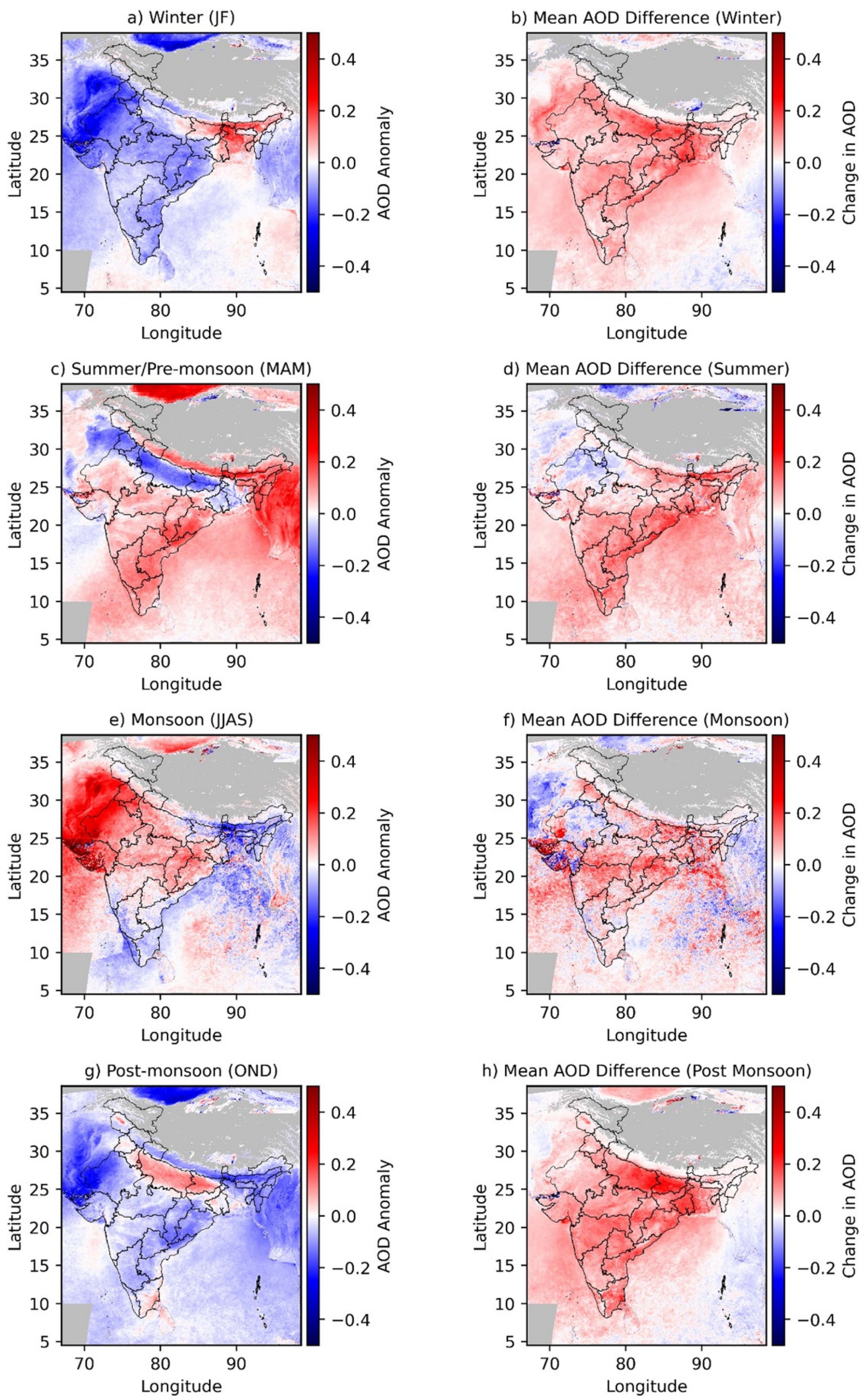

Figure 2. (a), (c), (e) and (g) are the seasonal AOD anomaly (seasonal AOD-annual AOD) plots with the annual average AOD for winter, summer, monsoon, and post-monsoon, respectively, for the second decade (2011–2019). (b), (d), (f) and (h) are the mean AOD decadal difference plots for the respective seasons. (Grey color represents missing data).

is seen across all regions, with the highest increase in the IGP (+0.06, 12%) and the eastern coastal region (+0.098, 25%). This marks an increasing trend in AOD in all urban, peri-urban, and rural regions.

Comparing the urban and peri-urban AOD across both decades reveals interesting trends (figure 3(c)). In the first decade, the central, western, eastern, and IGP regions exhibit slightly higher AOD in peri-urban areas, while the southern region shows a marginally higher AOD level in urban areas. In the second decade, the southern region and a few states in the central region experience a relatively higher increase in AOD in peri-urban areas. However, in the IGP, eastern, and western regions, urban AOD remains lower than those in peri-urban areas, and no significant change is seen in the difference in AOD

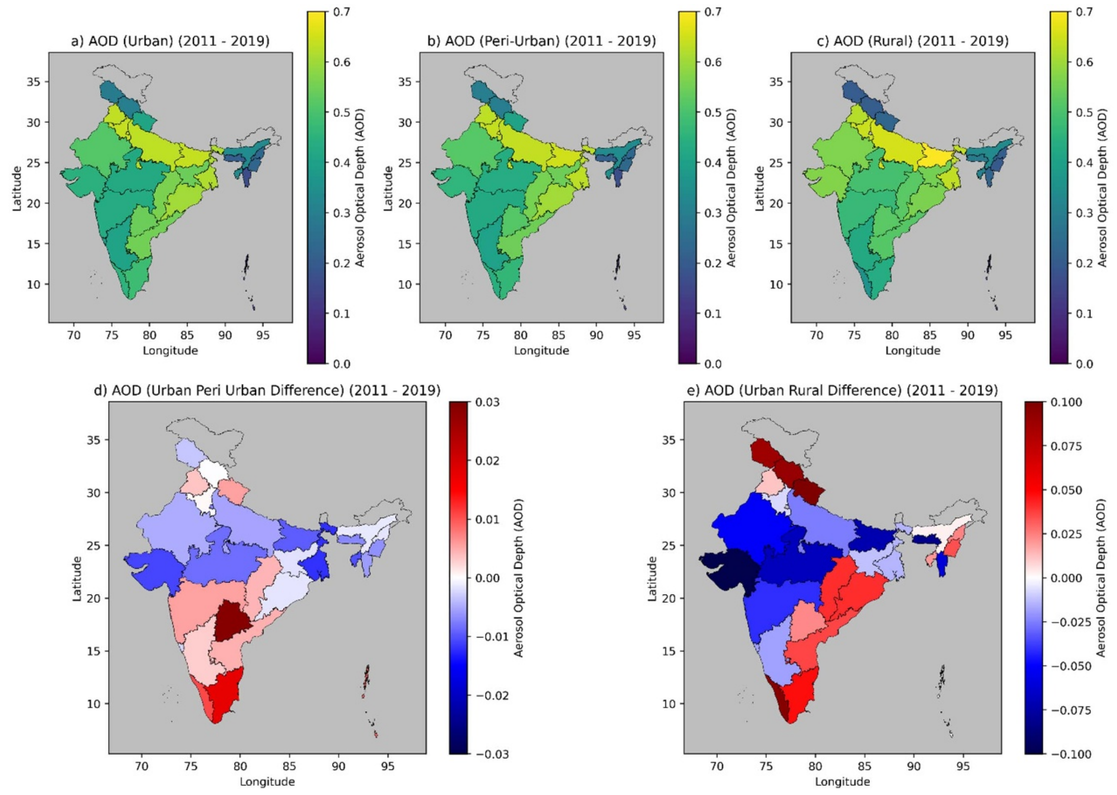

Figure 3. (a) State-wise area-weighted AOD average for urban regions for the year (2011–2019), (b) state-wise area-weighted AOD average for peri-urban regions for the year (2011–2019), (c) state-wise area-weighted AOD average for Rural regions for the year (2011–2019), (d) difference between Urban average AOD and peri-urban average AOD for the year (2011–2019), (e) difference between Urban average AOD and rural average AOD for the year (2011–2019). (Grey color represents missing data).

in both decades, although the difference increases in the southern region from +0.004 to +0.013. Overall, the number of states with a positive AOD difference (i.e. urban AOD greater than peri-urban AOD) increased from 10 to 13 out of 32 in the second decade. When comparing urban and rural AOD (figure 3(d)), the northern region and the eastern and southeastern coastal regions display higher AOD in urban areas compared to rural areas (ranging from 0.01 to 0.04), while the IGP, central, and western regions show a negative difference, i.e. lower AOD levels in urban areas with respect to the rural areas (ranging from 0.01 to 0.06). This pattern persists into the second decade but with a greater magnitude of difference in AOD. The northwest IGP region (Punjab and Haryana) and states like Maharashtra and Chhattisgarh show a shift from a negative to a positive difference in the second decade. Overall, the number of states with a positive difference decreased from 18 to 17 out of 32 in the second decade.

3.3. Association between AOD and ground-level PM

Finally, we examined associations between the AOD estimates from MODIS and the $PM_{2.5,\,g}$ concentration data for selected stations in three prominent urban centers: Delhi, Kanpur, and Mumbai (table S1 and figures 4(a)–(c)) across multiple time periods (figure S7). Some data points were excluded during data sanity checks using the AirPy tool (section 2.2) to fix errors like unit mismatches, repeated values, and invalid negative readings, and we got 2–3 years' worth of $PM_{2.5,\,g}$. Despite this reduction, we are able to compute the coefficient of determination (R^2), yielding a value of 0.61, indicating a high correlation between AOD and $PM_{2.5,\,g}$ concentrations (in figure 4(c)).

Notably, this correlation remains consistent across most locations in Kanpur and Delhi. However, in the case of Mumbai, we encounter challenges in establishing a similar relationship (figure S7). This discrepancy may be attributed to the limited dataset available post-cleaning, primarily due to clouds, which would also affect the satellite AOD retrievals, and particularly during the monsoon season.

Correlation analysis between changes in average AOD and $PM_{2.5,\,s}$ concentrations from 2001–2010–2011–2019 uncovers additional insights. The correlation graph (figure 4(d)) illustrates a discernible but variable correlation, with a coefficient of determination (R^2) of 0.49. This indicates a moderate correlation between AOD and $PM_{2.5,\,s}$, suggesting a degree of association between these parameters. Notably, the inclusion of Delhi and Haryana from the analysis significantly impacts the correlation, reducing the R^2 value to 0.19. This decline points to the substantial influence of these regions on the overall correlation,

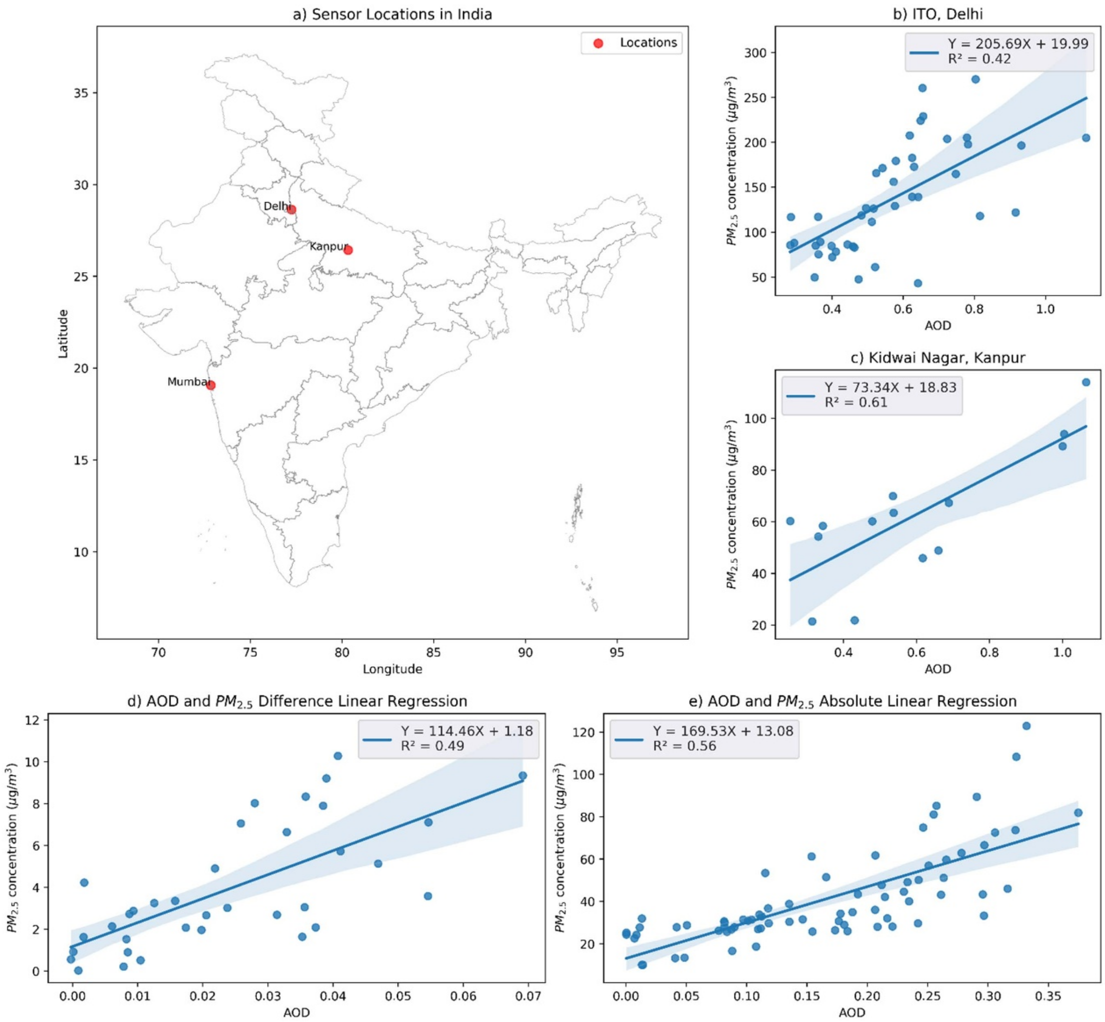

Figure 4. (a) The location of the cities from where the $PM_{2.5,\,g}$ data is taken, (b) and (c) the AOD vs $PM_{2.5,\,g}$ regression with the linear equation and their R^2 value, (d) the state-wise absolute difference from two decades of AOD vs $PM_{2.5,\,s}$ regression and (e) the state-wise absolute AOD and $PM_{2.5,\,s}$ regression for both decades.

likely due to their already elevated AOD and $PM_{2.5,\,s}$ levels.

4. Discussion and conclusion

This study highlights the shifts in aerosol pollution across India over the two decades between 2001 and 2019, with significant regional variations in AOD and $PM_{2.5}$ concentrations. The IGP consistently emerges as a region of concern due to its high AOD and air pollution, largely driven by a combination of anthropogenic activities and natural processes. Notably, agricultural crop burning has escalated by 2.35% annually, contributing to worsening air quality (Shaik *et al* 2019). The 21% population growth between 2001 and 2011, followed by a further 17% increase by 2019, has exacerbated pollution levels and corresponding population-level impacts (Mogno *et al* 2021). The IGP's aerosol load is shaped by local activities and environmental factors, including desert dust from the Thar Desert. Relatively lower boundary layer heights in the northeast traps aerosols, raising their concentration and AOD (figures S8 and S9). Additionally, increased wind speed (around 0.5 m s^{-1}) in the IGP during the second decade has led to post-monsoon anomalies and the spread of high AOD (figures S10–S12).

The southern region, despite showing lower AOD and $PM_{2.5,\,s}$ concentrations relative to northern areas, presents a clear gradient that correlates with population density and pollution sources. This north-south gradient reflects the significant impact of human activities in the northern region, which are amplified by geographic features like the Himalayas that trap pollutants (Dey and Di Girolamo 2010). On the other hand, the western region, particularly Rajasthan, demonstrates an anomaly, where despite low population density, AOD levels remain high. This phenomenon is largely attributed to the region's arid conditions, which promote dust dispersion by prevailing winds (Kumar *et al* 2017), although recent land cover changes, i.e. a decrease in barren lands may be reducing dust emissions (Dutta and Chatterjee 2022).

Seasonal variations are an integral part of the AOD dynamics. The seasonal anomaly, calculated as the annual average AOD subtracted from the seasonal average AOD, are shown as anomaly plots (figure 2). Winter and post-monsoon seasons show pronounced increases in AOD in the IGP, driven by biomass burning and meteorological conditions that limit dispersion. In contrast, during the monsoon, aerosol loads decrease across most regions due to heavy rainfall that scavenges particles from the atmosphere. These seasonal fluctuations underscore the complex interplay between natural and anthropogenic sources and meteorological factors in shaping AOD patterns. The post-monsoon period, in particular, stands out due to the sharp rise in AOD in the IGP, linked to peak agricultural burning during this time.

In winter, AOD levels are generally lower than the annual average across southern, central, and western IGP regions, except in the eastern IGP and northeast, where forest fires (density around 500 fire points per 0.5×0.5 grid) raise AOD (Shaik *et al* 2019). In summer, increased fire activity in the southern peninsula (density: 200–500 fire points in 0.5×0.5 grid) and wheat residue burning in Punjab and Haryana (density > 1000) contribute to AOD anomalies, but summer AOD remains below the annual average due to the higher post-monsoon paddy season fire counts, which account for 77% of total fires in Punjab and Haryana. The monsoon season sees negligible biomass burning, and rainfall lowers AOD in the southern and northeastern regions. Post-monsoon, AOD rises sharply in the IGP due to peak biomass burning and increased wind speeds, further spreading aerosols.

A distinctive feature of this study is its examination of AOD differences across urban, peri-urban, and rural areas (figure 4). The findings suggest that the differences in AOD between urban and peri-urban areas are minimal, indicating that advection plays a significant role in distributing aerosols, thus moderating spatial contrasts in air quality. However, rural regions, particularly in the western and IGP regions, show higher AOD levels compared to urban areas, which is likely due to external sources like dust storms and biomass burning. The second decade of the study reveals an increase in the magnitude of AOD differences between rural and urban areas, with peri-urban regions often serving as a transition zone where external pollution sources exert greater influence.

The relationship between satellite-derived AOD and $PM_{2.5,\,g}$ is critical for understanding air quality in regions with sparse ground monitoring networks. This study shows that while AOD generally captures long-term $PM_{2.5}$ trends, the strength of the correlation varies across regions. In Kanpur, a strong correlation ($R^2 = 0.61$) was observed, whereas regions like Mumbai, with complex meteorological conditions and limited data due to cloud cover, exhibited weaker correlations. These findings highlight the limitations of satellite-derived AOD as a standalone proxy for $PM_{2.5}$, particularly in coastal and cloud-covered regions. Nevertheless, AOD remains a valuable tool for assessing air quality trends, especially in areas lacking sufficient ground-based monitoring infrastructure.

The study underscores the need for enhanced monitoring and mitigation efforts, especially in regions like the IGP, where both population growth and industrial activities are expected to continue rising. As AOD trends demonstrate the long-term impact of both human and environmental factors on air quality, future efforts must integrate satellite observations with ground-based measurements to provide more accurate and comprehensive assessments of pollution levels. This will be crucial for managing air quality and mitigating public health risks in India's most vulnerable regions.

Data availability statement

All data developed for this study will be available from the corresponding authors on request.

Acknowledgment

TC's contribution was supported by the US Department of Energy, Office of Science, Biological and Environmental Research programme through an Early Career award. Pacific Northwest National Laboratory is operated for the US Department of Energy by Battelle Memorial Institute under Contract Number DE-AC05-76RL01830.

ORCID iDs

TC Chakraborty https://orcid.org/0000-0003-1338-3525

Abhishek Chakraborty https://orcid.org/0000-0001-9531-6419

References

CCR 2023 *Central Control Room for Air Quality Management—All India* (available at: https://app.cpcbccr.com/ccr/#/caaqm-dashboard-all/caaqm-landing)

Chakraborty T and Lee X 2019 A simplified urban-extent algorithm to characterize surface urban heat islands on a global scale and examine vegetation control on their spatiotemporal variability *Int. J. Appl. Earth Obs. Geoinf.* **74** 269–80

Chakraborty T, Sarangi C and Lee X 2021 Reduction in human activity can enhance the urban heat island: insights from the COVID-19 lockdown *Environ. Res. Lett.* **16** 054060

Choudhry P, Misra A and Tripathi S N 2012 Study of MODIS derived AOD at three different locations in the Indo Gangetic Plain: kanpur, Gandhi College and Nainital *Ann. Geophys.* **30** 1479–93

CPCB 2023 *CPCB | National Ambient Air Quality Monitoring Series* (available at: https://cpcb.nic.in/publication-details.php?pid=OA==)

Dey S *et al* 2020 A satellite-based high-resolution (1-km) ambient $PM_{2.5}$ database for India over two decades (2000–2019):

applications for air quality management *Remote Sens.* **12** 3872
Dey S and Di Girolamo L 2010 A climatology of aerosol optical and microphysical properties over the Indian subcontinent from 9 years (2000–2008) of Multiangle Imaging Spectroradiometer (MISR) data *J. Geophys. Res.* **115** D15204
Dutta M and Chatterjee A 2022 A deep insight into state-level aerosol pollution in India: long-term (2005–2019) characteristics, source apportionment, and future projection (2023) *Atmos. Environ.* **289** 119312
Fenger J 1999 Urban air quality *Atmos. Environ.* **33** 4877–900
Goel A, Wathore R, Chakraborty T and Agrawal M 2017 Characteristics of exposure to particles due to incense burning inside temples in Kanpur, India *Aerosol Air Qual. Res.* **17** 608–15
Gorelick N, Hancher M, Dixon M, Ilyushchenko S, Thau D and Moore R 2017 Google earth engine: planetary-scale geospatial analysis for everyone *Remote Sens. Environ.* **202** 18–27
Indian Meteorological Department, GOI 2023 *Indian Meteorological Department* (Indian Meteorological Department) (available at: https://mausam.imd.gov.in/responsive/subDivisionWiseWarning.php)
Kumar R, Mishra V, Buzan J, Kumar R, Shindell D and Huber M 2017 Dominant control of agriculture and irrigation on urban heat island in India *Sci. Rep.* **7** 14054
Lee H J, Liu Y, Coull B A, Schwartz J and Koutrakis P 2011 A novel calibration approach of MODIS AOD data to predict $PM_{2.5}$ concentrations *Atmos. Chem. Phys.* **11** 7991–8002
Lyapustin A and Wang Y 2022 *MODIS/Terra+Aqua Land Aerosol Optical Depth Daily L2G Global 1km SIN Grid V061* (NASA EOSDIS Land Processes Distributed Active Archive Center) (https://doi.org/10.5067/MODIS/MCD19A2.061)
Madhumitha C *et al* 2023 Urgent issues regarding real-time air quality monitoring data in India: unveiling solutions and implications for policy and health *Atmos. Environ.* X *Under review*
Mogno C, Palmer P I, Knote C, Yao F and Wallington T J 2021 Seasonal distribution and drivers of surface fine particulate matter and organic aerosol over the Indo-Gangetic Plain *Atmos. Chem. Phys.* **21** 10881–909
Musonda B, Jing Y, Nyasulu M and Libanda B 2022 Long-term spatial and temporal variations of aerosol optical depth during 2000–2020 over Zambia, southcentral Africa *Air Qual. Atmos. Health* **15** 177–93
Open Government Data (OGD) Platform India 2022 *Sub Divisional Monthly Rainfall from 1901 to 2017* (available at: https://data.gov.in/resource/sub-divisional-monthly-rainfall-1901-2017)
Ramachandran S and Kedia S 2013 Aerosol optical properties over south asia from ground-based observations and remote sensing: a review *Climate* **1** 84–119
Ramachandran S, Kedia S and Srivastava R 2012 Aerosol optical depth trends over different regions of India *Atmos. Environ.* **49** 338–47
Ranjan A K, Patra A K and Gorai A K 2021 A review on estimation of particulate matter from satellite-based aerosol optical depth: data, methods, and challenges *Asia-Pac. J. Atmos.* **57** 679–99
Rawat P, Sarkar S, Jia S, Khillare P S and Sharma B 2019 Regional sulfate drives long-term rise in AOD over megacity Kolkata, India *Atmos. Environ.* **209** 167–81
Sarthi P P, Kumar S, Barat A, Kumar P, Sinha A K and Goswami V 2019 Linkage of aerosol optical depth with rainfall and circulation parameters over the Eastern Gangetic Plains of India *J. Earth Syst. Sci.* **128** 171
Shaik D S, Kant Y, Mitra D, Singh A, Chandola H C, Sateesh M, Babu S S and Chauhan P 2019 Impact of biomass burning on regional aerosol optical properties: a case study over northern India *J. Environ. Manage.* **244** 328–43
Sharma D and Kulshrestha U C 2014 Spatial and temporal patterns of air pollutants in rural and urban areas of India *Environ. Pollut.* **195** 276–81
Vadrevu K P, Ellicott E, Badarinath K V S and Vermote E 2011 MODIS derived fire characteristics and aerosol optical depth variations during the agricultural residue burning season, north India *Environ. Pollut.* **159** 1560–9
Van Donkelaar A *et al* 2021 Monthly global estimates of fine particulate matter and their uncertainty *Environ. Sci. Technol.* **55** 15287–300
Vohra K *et al* 2021 Long-term trends in air quality in major cities in the UK and India: a view from space *Atmos. Chem. Phys.* **21** 6275–96